

Tethered silyl complexes from nucleophilic substitution reactions at the Si–Cl bond of the chloro(diphenyl)silyl ligand in $\text{Ru}(\text{SiClPh}_2)(\kappa^2\text{-S}_2\text{CNMe}_2)(\text{CO})(\text{PPh}_3)_2$

Wai-Him Kwok, Guo-Liang Lu, Clifton E.F. Rickard,
Warren R. Roper*, L. James Wright*

Department of Chemistry, The University of Auckland, P.O. Bag 92019, Auckland, New Zealand

Received 14 April 2004; accepted 10 June 2004

Available online 6 August 2004

Abstract

Crystal structure determination of $\text{RuH}(\kappa^2\text{-S}_2\text{CNMe}_2)(\text{CO})(\text{PPh}_3)_2$ (**1**) confirms that the triphenylphosphine ligands are arranged mutually *trans*. **1** reacts readily with HSiClPh_2 to eliminate H_2 and produce the six-coordinate silyl complex, $\text{Ru}(\text{SiClPh}_2)(\kappa^2\text{-S}_2\text{CNMe}_2)(\text{CO})(\text{PPh}_3)_2$ (**2**). Crystal structure determination of **2** reveals the same geometrical arrangement of ligands as in **1** with the silyl ligand replacing the hydride ligand. The chloride bound to silicon in **2** is replaced through reactions with 2-hydroxypyridine, 2-aminopyridine, and thallium acetate, producing, respectively, the mono- PPh_3 complexes, $\text{Ru}(\kappa^2(\text{Si},\text{N})\text{-SiPh}_2\text{OC}_5\text{H}_4\text{N})(\kappa^2\text{-S}_2\text{CNMe}_2)(\text{CO})(\text{PPh}_3)$ (**3**), $\text{Ru}(\kappa^2(\text{Si},\text{N})\text{-SiPh}_2\text{NHC}_5\text{H}_4\text{N})(\kappa^2\text{-S}_2\text{CNMe}_2)(\text{CO})(\text{PPh}_3)$ (**4**), and $\text{Ru}(\kappa^2(\text{Si},\text{O})\text{-SiPh}_2\text{OCMeO})(\kappa^2\text{-S}_2\text{CNMe}_2)(\text{CO})(\text{PPh}_3)$ (**5**). Crystal structure determinations of **3**, **4**, and **5** confirm that in each case there is formation of a five-membered chelate ring tethering the silyl ligand to ruthenium. In the formation of **3**, **4**, and **5** the Si-ligand and the two S atoms of the dimethyldithiocarbamate ligand remain meridional but the remaining triphenylphosphine ligand and the carbonyl ligand are interchanged in position leaving the donor atom of the tether *trans* to the CO ligand. An alternative way of considering the tethered silyl ligands in **3**, **4**, and **5** is as tethered, base-stabilised, silylene ligands and the structural data give some support for a contribution from this bonding model.

© 2004 Elsevier B.V. All rights reserved.

Keywords: Silyl complex; Ruthenium; X-ray crystal structure; Bidentate ligand

1. Introduction

Metal complexes containing chloro-substituted silyl ligands, $\text{L}_n\text{M-SiR}_{3-n}\text{Cl}_n$ ($n=1-3$), have proved to be useful substrates, through nucleophilic substitution reactions at the Si–Cl bonds, for the synthesis of a wide range of silyl complexes with interestingly functionalised silyl ligands [1]. The reactivity of the Si–Cl bonds in all chlorosilyl ligands is variable, and not particularly pre-

dictable, but two trends which have emerged are that more electron-rich metal centers reduce the reactivity of the Si–Cl bonds [2] while coordinative unsaturation at the metal increases the reactivity of the Si–Cl bonds [1d]. To contribute to further understanding of the reactivity of chloro-substituted silyl ligands we have developed a convenient route to a coordinatively saturated chloro(diphenyl)silyl complex of ruthenium(II) and examined some features of its chemistry.

Herein, we report (i) the synthesis of $\text{Ru}(\text{SiClPh}_2)(\kappa^2\text{-S}_2\text{CNMe}_2)(\text{CO})(\text{PPh}_3)_2$ (**2**) from $\text{RuH}(\kappa^2\text{-S}_2\text{CNMe}_2)(\text{CO})(\text{PPh}_3)_2$ (**1**) and HSiClPh_2 , (ii) the reactions of the Si–Cl bond in **2** with 2-hydroxypyridine, 2-aminopyridine, or thallium acetate which lead to the tethered silyl

* Corresponding authors. Tel.: +64-9-373-7999x8320; fax: +64-9-373-7422.

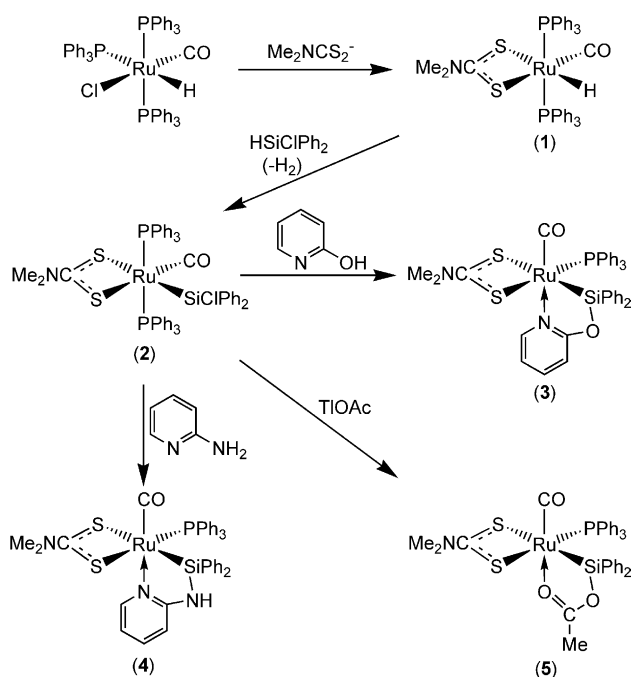
E-mail address: w.roper@auckland.ac.nz (W.R. Roper).

complexes, $\text{Ru}(\kappa^2(\text{Si},\text{N})\text{-SiPh}_2\text{OC}_5\text{H}_4\text{N})(\kappa^2\text{-S}_2\text{CNMe}_2)(\text{CO})(\text{PPh}_3)_2$ (**3**), $\text{Ru}(\kappa^2(\text{Si},\text{N})\text{-SiPh}_2\text{NHC}_5\text{H}_4\text{N})(\kappa^2\text{-S}_2\text{CNMe}_2)(\text{CO})(\text{PPh}_3)_2$ (**4**), or $\text{Ru}(\kappa^2(\text{Si},\text{O})\text{-SiPh}_2\text{OCMeO})(\kappa^2\text{-S}_2\text{CNMe}_2)(\text{CO})(\text{PPh}_3)_2$ (**5**), respectively, and (iii) the crystal structure determinations of complexes **1–5**.

2. Results and discussion

2.1. Synthesis of $\text{Ru}(\text{SiClPh}_2)(\kappa^2\text{-S}_2\text{CNMe}_2)(\text{CO})(\text{PPh}_3)_2$ (**2**) from $\text{RuH}(\kappa^2\text{-S}_2\text{CNMe}_2)(\text{CO})(\text{PPh}_3)_2$ (**1**) and the structures of (**1**) and (**2**)

As depicted in Scheme 1, reaction between $\text{RuH}(\kappa^2\text{-S}_2\text{CNMe}_2)(\text{CO})(\text{PPh}_3)_2$ (**1**) and a 10-fold excess HSiClPh_2 , leads to pale yellow $\text{Ru}(\text{SiClPh}_2)(\kappa^2\text{-S}_2\text{CNMe}_2)(\text{CO})(\text{PPh}_3)_2$ (**2**) in high yield. The IR spectrum of **2** shows a $\nu(\text{CO})$ band at 1915 cm^{-1} which is slightly lower than the value of 1920 cm^{-1} reported for **1** [3]. In the ^1H NMR spectrum two resonances are seen for the inequivalent methyl groups of the dithiocarbamate ligand at 2.16 and 2.35 ppm. This is consistent with the structure shown in Scheme 1 which has been confirmed by crystal structure determination (see below). The geometry of **2** is therefore the same as **1** with the silyl ligand replacing the hydride ligand. For the purpose of a close structural comparison of all the Ru-ligand bond distances in these two compounds the structures of both **1** and **2** were determined. Crystal data and refinement details for **1**, **2**, and all other structures reported in this paper, are given in Table 1.



Scheme 1. Synthesis and reactions of the chloro(diphenyl)silyl complex, $\text{Ru}(\text{SiClPh}_2)(\kappa^2\text{-S}_2\text{CNMe}_2)(\text{CO})(\text{PPh}_3)_2$ (**2**).

For **1** and **2**, the molecular structures are shown in Figs. 1 and 2, and selected bond lengths and angles are given in Tables 2 and 3, respectively. The geometry of both complexes is octahedral with the two triphenylphosphine ligands arranged mutually *trans*. The Ru–H distance in **1** is 1.718(18) Å and this can be compared with the average (1.581 with SD 0.119 Å) of 360 measured distances recorded in the Cambridge Crystallographic Data Base. The attachment of the bidentate dimethyldithiocarbamate ligand is unsymmetrical for both **1** and **2** with the Ru–S distances greater when S is *trans* to the hydride ligand in **1** and to the silyl ligand in **2**. The Ru–S distances *trans* to CO are almost identical (Ru–S, 2.4568(10) Å for **1** and 2.4598(7) Å for **2**). Based on the Ru–S distances the *trans* influence of the silyl ligand is slightly greater than the hydride ligand in these complexes (Ru–S, 2.4884(9) Å for **1** and 2.4980(7) Å for **2**). The Ru–P distances in **1** (2.3328(9) and 2.3784(9) Å) are considerably less than the Ru–P distances in **2** (2.3985(7) and 2.4112(7) Å), presumably reflecting the lesser steric demands of the hydride ligand compared to the silyl ligand. The Ru–Si distance in **2** is 2.4089(7) Å, which is very close to the average (2.4035 with SD 0.0478 Å) of 44 measured distances recorded in the Cambridge Crystallographic Data Base for octahedral ruthenium silyl complexes where silicon is four-coordinate. The Si–Cl distance is 2.1518(10) Å, which is remarkably long when compared with the average of recorded Si–Cl distances of 2.0579 Å, SD 0.0435 Å (Cambridge Crystallographic Data Base). Another unusual feature associated with the Si–Cl bond is that the angle Ru–Si–Cl is less than tetrahedral (107.87(4)°) whereas the Ru–Si–phenyl angles are 119.18 and 124.51°. This less-than-tetrahedral angle for Ru–Si–Cl and much greater-than-tetrahedral angles for Ru–Si–phenyl, has the effect of “flattening” the arrangement of Ru and the two phenyl substituents on Si (sum of angles 345.23°). This effect is even more accentuated in the structures **3**, **4**, and **5** discussed below. Other chloro(diphenyl)silyl complexes all have M–Si–Cl angles greater than tetrahedral [4] except for $\text{CpFe}(\text{CO})_2\text{SiPh}(\text{C}_6\text{H}_4\text{OMe}-2)\text{Cl}$ where the angle Fe–Si–Cl is 108.09(3)° [1h].

2.2. Nucleophilic substitution at the Si–Cl bond of **2** by 2-hydroxypyridine, 2-aminopyridine, and acetate, to give the corresponding tethered silyl complexes $\text{Ru}(\kappa^2(\text{Si},\text{N})\text{-SiPh}_2\text{OC}_5\text{H}_4\text{N})(\kappa^2\text{-S}_2\text{CNMe}_2)(\text{CO})(\text{PPh}_3)$ (**3**), $\text{Ru}(\kappa^2(\text{Si},\text{N})\text{-SiPh}_2\text{NHC}_5\text{H}_4\text{N})(\kappa^2\text{-S}_2\text{CNMe}_2)(\text{CO})(\text{PPh}_3)$ (**4**), and $\text{Ru}(\kappa^2(\text{Si},\text{O})\text{-SiPh}_2\text{OCMeO})(\kappa^2\text{-S}_2\text{CNMe}_2)(\text{CO})(\text{PPh}_3)$ (**5**)

As shown in Scheme 1 complex **2** reacts readily with 2-hydroxypyridine, 2-aminopyridine, and thallium acetate to give, in good yield, the colourless, tethered, silyl complexes $\text{Ru}(\kappa^2(\text{Si},\text{N})\text{-SiPh}_2\text{OC}_5\text{H}_4\text{N})(\kappa^2\text{-S}_2\text{CNMe}_2)(\text{CO})(\text{PPh}_3)$ (**3**), $\text{Ru}(\kappa^2(\text{Si},\text{N})\text{-SiPh}_2\text{NHC}_5\text{H}_4\text{N})(\kappa^2\text{-S}_2\text{CNMe}_2)(\text{CO})(\text{PPh}_3)$ (**4**), and $\text{Ru}(\kappa^2(\text{Si},\text{O})\text{-SiPh}_2\text{OCMeO})(\kappa^2\text{-S}_2\text{CNMe}_2)(\text{CO})(\text{PPh}_3)$ (**5**).

Table 1
Data collection and processing parameters for 1–5

	1	2	3·2.5C ₆ H ₆	4	5·CH ₂ Cl ₂
Formula	C ₄₀ H ₃₇ NOP ₂ RuS ₂	C ₅₂ H ₄₆ ClNOP ₂ RuS ₂ Si	C ₅₄ H ₅₀ N ₂ O ₂ PRuS ₂ Si	C ₃₉ H ₃₆ N ₃ OPRuS ₂ Si	C ₃₇ H ₃₆ Cl ₂ NO ₃ PRuS ₂ Si
Molecular weight	774.84	991.57	983.21	786.96	837.82
Crystal system	Monoclinic	Monoclinic	Triclinic	Monoclinic	Monoclinic
Space group	<i>P</i> 2 ₁ / <i>c</i>	<i>P</i> 2 ₁ / <i>c</i>	<i>P</i> $\bar{1}$	<i>P</i> 2 ₁ / <i>c</i>	<i>C</i> 2/ <i>c</i>
<i>a</i> (Å)	13.4658(2)	10.2887(1)	11.7848(1)	10.6009(1)	40.9807(4)
<i>b</i> (Å)	15.4931(2)	21.8567(3)	12.1648(1)	17.8163(1)	10.1942(1)
<i>c</i> (Å)	18.5896(2)	20.7550(2)	19.3655(1)	19.3417(1)	23.1315(4)
α (°)	90.0	90.0	107.160(1)	90.0	90.0
β (°)	110.048(1)	93.151(1)	94.832(1)	97.622(1)	121.310(1)
γ (°)	90.0	90.0	111.388(1)	90.0	90.0
<i>V</i> (Å ³)	3643.29(8)	4660.27(9)	2411.86	3620.77(4)	8256.39(18)
<i>Z</i>	4	4	2	4	8
<i>d</i> (calc) (g cm ⁻³)	1.413	1.413	1.354	1.444	1.348
<i>F</i> (000)	1592	2040	1018	1616	3424
μ (mm ⁻¹)	0.66	0.62	0.51	0.66	0.71
Crystal size (mm)	0.44×0.18×0.14	0.45×0.36×0.18	0.43×0.33×0.21	0.38×0.28×0.21	0.38×0.08×0.07
2 θ (min–max) (°)	1.6–27.5	1.4–27.4	1.8–27.5	1.5–27.5	1.7–25.0
Reflections collected	20,768	26,184	23,323	21,981	23,124
Independent reflections	7952 <i>R</i> _{int} = 0.0349	10,138 <i>R</i> _{int} = 0.0265	10,357 <i>R</i> _{int} = 0.0158	8002 <i>R</i> _{int} = 0.0217	8068 <i>R</i> _{int} = 0.0674
<i>A</i> (min–max)	0.758–0.913	0.768–0.897	0.809–0.900	0.787–0.874	0.774–0.952
Goodness-of-fit on <i>F</i> ²	1.081	1.074	1.018	1.102	1.001
<i>R</i> (observed data)	<i>R</i> ₁ = 0.0461, <i>wR</i> ₂ = 0.0956	<i>R</i> ₁ = 0.0363, <i>wR</i> ₂ = 0.0706	<i>R</i> ₁ = 0.0257, <i>wR</i> ₂ = 0.0639	<i>R</i> ₁ = 0.0364, <i>wR</i> ₂ = 0.0872	<i>R</i> ₁ = 0.0576, <i>wR</i> ₂ = 0.1396
<i>R</i> (all data)	<i>R</i> ₁ = 0.0694, <i>wR</i> ₂ = 0.1058	<i>R</i> ₁ = 0.0523, <i>wR</i> ₂ = 0.0773	<i>R</i> ₁ = 0.0304, <i>wR</i> ₂ = 0.0667	<i>R</i> ₁ = 0.0471, <i>wR</i> ₂ = 0.0944	<i>R</i> ₁ = 0.0880, <i>wR</i> ₂ = 0.1535
Diff. map (min–max) (e Å ⁻³)	1.14–1.00	0.44–0.40	0.61–0.49	0.63–0.46	2.22–1.08

$$R = \sum \| |F_o| - |F_c| \| / \sum |F_o|, \quad wR_2 = \{ \sum [w(F_o^2 - F_c^2)^2] / \sum [w(F_o^2)^2] \}^{1/2}.$$

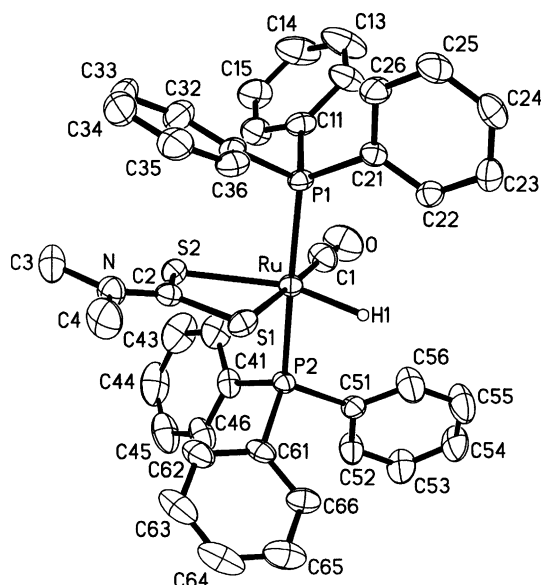


Fig. 1. Molecular geometry of $\text{RuH}(\kappa^2\text{-S}_2\text{CNMe}_2)(\text{CO})(\text{PPh}_3)_2$ (**1**).

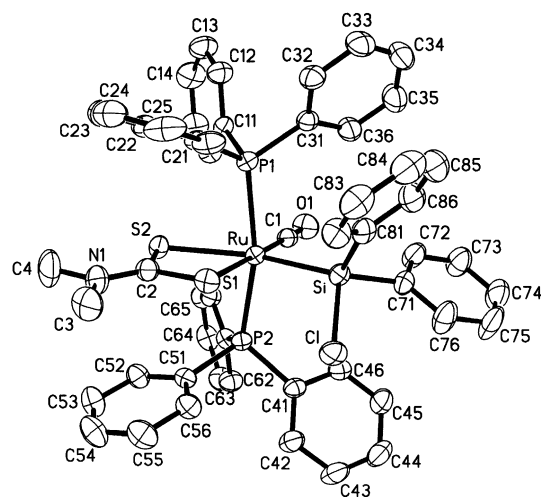


Fig. 2. Molecular geometry of $\text{Ru}(\text{SiClPh}_2)(\kappa^2\text{-S}_2\text{CNMe}_2)(\text{CO})(\text{PPh}_3)_2$ (**2**).

$(\text{CO})(\text{PPh}_3)$ (**3**), $\text{Ru}(\kappa^2(\text{Si},\text{N})\text{-SiPh}_2\text{NHC}_5\text{H}_4\text{N})(\kappa^2\text{-S}_2\text{-CNMe}_2)(\text{CO})(\text{PPh}_3)$ (**4**), and $\text{Ru}(\kappa^2(\text{Si},\text{O})\text{-SiPh}_2\text{OCMe-O})(\kappa^2\text{-S}_2\text{CNMe}_2)(\text{CO})(\text{PPh}_3)$ (**5**), respectively. In each reaction a triphenylphosphine ligand is lost and there is a rearrangement of the coordination sphere in that the remaining triphenylphosphine ligand, which was originally in a facial configuration with the two sulfur atoms of the chelating dimethyldithiocarbamate ligand, is now found in a meridional configuration with the two S atoms. At the same time the CO ligand moves from a meridional arrangement with respect to the two S atoms to one in which this arrangement becomes facial. The IR spectra of **3**, **4**, and **5** show $\nu(\text{CO})$ bands at 1915, 1925, and 1909 cm^{-1} , respectively. The ^1H NMR spectrum of **4** shows a resonance at 5.15 ppm assigned to the

Table 2
Selected bond lengths (Å) and angles (°) for **1**

Bond lengths	
Ru–C(1)	1.859(5)
Ru–P(2)	2.3328(9)
Ru–P(1)	2.3784(9)
Ru–S(1)	2.4568(10)
Ru–S(2)	2.4884(9)
Ru–H(1)	1.718(18)
S(1)–C(2)	1.716(4)
S(2)–C(2)	1.714(4)
N–C(2)	1.333(4)
N–C(4)	1.463(5)
N–C(3)	1.465(5)
Bond angles	
C(1)–Ru–P(2)	85.95(13)
C(1)–Ru–P(1)	89.77(13)
P(2)–Ru–P(1)	175.68(3)
C(1)–Ru–S(1)	178.19(13)
P(2)–Ru–S(1)	95.55(3)
P(1)–Ru–S(1)	88.72(3)
C(1)–Ru–S(2)	107.74(14)
P(2)–Ru–S(2)	91.27(3)
P(1)–Ru–S(2)	89.48(3)
S(1)–Ru–S(2)	71.25(3)
C(1)–Ru–H(1)	94.3(12)
P(2)–Ru–H(1)	83.8(11)
P(1)–Ru–H(1)	97.1(11)
S(1)–Ru–H(1)	86.9(12)
S(2)–Ru–H(1)	157.1(12)

NH function. In the ^{13}C NMR spectra of **4** and **5** a doublet signals for the CO ligands are seen at 204.9 ppm ($^2J_{\text{CP}} = 16.1$ Hz) and at 204.7 ppm ($^2J_{\text{CP}} = 16.1$ Hz), respectively. For **3** the CO signal was seen at 204.6 ppm but the coupling to phosphorus was not resolved.

2.3. Structure determinations of the tethered silyl complexes **3**, **4**, and **5**

The molecular geometries of the complexes **3**, **4**, and **5** are shown in Figs 3–5, respectively. Selected bond lengths and angles are presented in Tables 4–6. The geometry of all three complexes is octahedral. The attachment of the bidentate dimethyldithiocarbamate ligand is again unsymmetrical for all three compounds with the Ru–S distances greater when S is *trans* to the silyl ligand (**3**, 2.5296(4); **4**, 2.5189(7); **5**, 2.4940(13) Å). The smaller Ru–S distances *trans* to PPh_3 are (**3**, 2.4529(4); **4**, 2.4374(7); **5**, 2.4249(12) Å). The Ru–Si distances for **3** (2.3487(4) Å), **4** (2.3400(7) Å), and **5** (2.3499(13) Å) are all considerably shortened with respect to the parent complex **2** (2.4089(7) Å). This can probably be attributed mainly to the formation of the favourable five-membered chelate ring but some contribution from possible silylene character in this bond should not be ignored. This is also suggested by the “flattening” of the two phenyl substituents and the bond to Ru, about Si. The sum

Table 3
Selected bond lengths (Å) and angles (°) for **2**

Bond lengths	
Ru–C(1)	1.845(2)
Ru–P(1)	2.3985(7)
Ru–Si	2.4089(7)
Ru–P(2)	2.4112(7)
Ru–S(1)	2.4598(7)
Ru–S(2)	2.4980(7)
Cl–Si	2.1518(10)
Si–C(81)	1.910(3)
Si–C(71)	1.914(3)
S(1)–C(2)	1.714(3)
S(2)–C(2)	1.725(3)
N(1)–C(2)	1.326(3)
N(1)–C(4)	1.461(4)
N(1)–C(3)	1.468(4)
O(1)–C(1)	1.159(3)

Bond angles	
C(1)–Ru–P(1)	88.14(8)
C(1)–Ru–Si	92.53(8)
P(1)–Ru–Si	99.65(2)
C(1)–Ru–P(2)	89.55(8)
P(1)–Ru–P(2)	163.94(2)
Si–Ru–P(2)	96.33(2)
C(1)–Ru–S(1)	179.39(8)
P(1)–Ru–S(1)	91.97(2)
Si–Ru–S(1)	88.04(2)
P(2)–Ru–S(1)	90.17(2)
C(1)–Ru–S(2)	108.31(8)
P(1)–Ru–S(2)	82.50(2)
Si–Ru–S(2)	159.14(2)
P(2)–Ru–S(2)	83.15(2)
S(1)–Ru–S(2)	71.12(2)
C(81)–Si–C(71)	101.54(12)
C(81)–Si–Cl	97.68(9)
C(71)–Si–Cl	101.64(9)
C(81)–Si–Ru	119.18(9)
C(71)–Si–Ru	124.51(8)
Cl–Si–Ru	107.87(4)

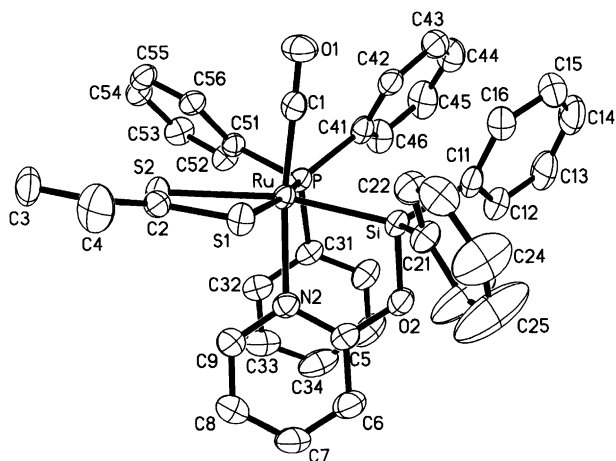


Fig. 3. Molecular geometry of $\text{Ru}(\kappa^2(\text{Si},\text{N})\text{-SiPh}_2\text{OC}_5\text{H}_4\text{N})(\kappa^2\text{-S}_2\text{CNMe}_2)(\text{CO})(\text{PPh}_3)$ (**3**) (only one enantiomer is shown).

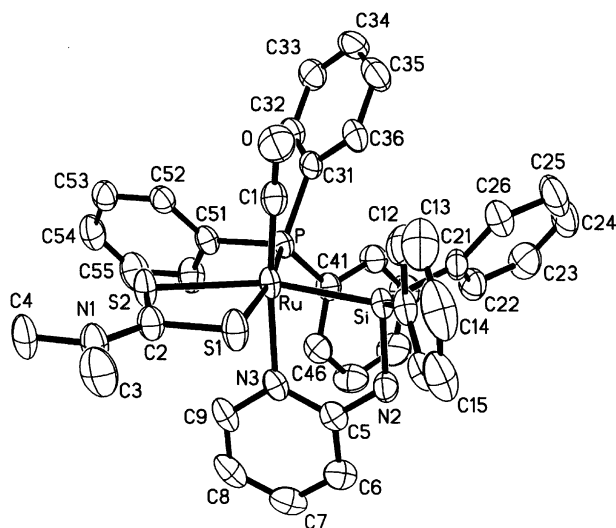


Fig. 4. Molecular geometry of $\text{Ru}(\kappa^2(\text{Si},\text{N})\text{-SiPh}_2\text{NHC}_5\text{H}_4\text{N})(\kappa^2\text{-S}_2\text{CNMe}_2)(\text{CO})(\text{PPh}_3)$ (**4**) (only one enantiomer is shown).

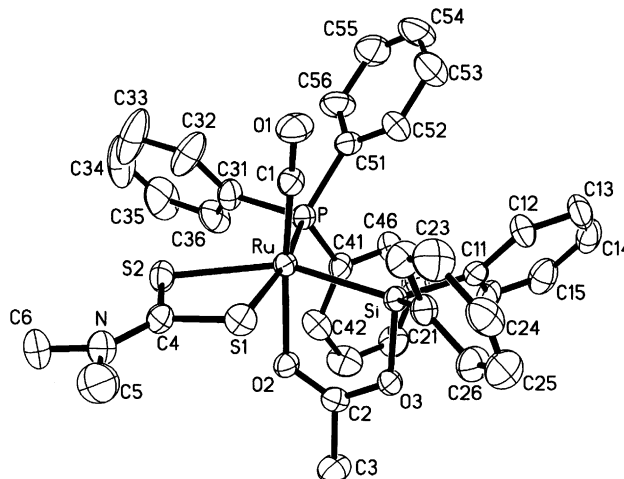


Fig. 5. Molecular geometry of $\text{Ru}(\kappa^2(\text{Si},\text{O})\text{-SiPh}_2\text{OCMeO})(\kappa^2\text{-S}_2\text{CNMe}_2)(\text{CO})(\text{PPh}_3)$ (**5**) (only one enantiomer is shown).

of the angles Ru–Si–phenyl, Ru–Si–phenyl, and phenyl–Si–phenyl is ca. 347° for **3**, 346° for **4**, 351° for **5**. In addition the measured Si–O and Si–N distances are exceptionally long. The average of all reported Si–O distances for four-coordinate Si is 1.6295 (SD 0.0334) Å (Cambridge Crystallographic Data Base), but the Si–O distance for **3** is 1.7333(13) Å and for **5** is 1.775(3) Å. Likewise, the average of all reported Si–N distances for four-coordinate Si is 1.7363 (SD 0.0378) Å (Cambridge Crystallographic Data Base), but the Si–N distance for **4** is 1.776(2) Å. The data above suggest that the base-stabilised silylene structure (A) shown in Scheme 2 could be a contributor to the bonding in complex **5**. Similar valence bond representations could be written for complexes **3** and **4**. The C–O distances within the acetate group suggest that there is more double bond

Table 4
Selected bond lengths (Å) and angles (°) for **3**

<i>Bond lengths</i>	
Ru–C(1)	1.8269(17)
Ru–N(2)	2.2167(14)
Ru–P	2.3409(4)
Ru–Si	2.3487(4)
Ru–S(1)	2.4529(4)
Ru–S(2)	2.5296(4)
Si–O(2)	1.7333(13)
Si–C(11)	1.8857(18)
Si–C(21)	1.8946(18)
S(1)–C(2)	1.7271(17)
S(2)–C(2)	1.7209(17)
O(1)–C(1)	1.159(2)
O(2)–C(5)	1.337(2)
N(1)–C(2)	1.328(2)
N(1)–C(4)	1.462(2)
N(1)–C(3)	1.465(2)
<i>Bond angles</i>	
C(1)–Ru–N(2)	170.81(6)
C(1)–Ru–P	92.44(5)
N(2)–Ru–P	92.15(4)
C(1)–Ru–Si	93.98(5)
N(2)–Ru–Si	77.60(4)
P–Ru–Si	96.251(16)
C(1)–Ru–S(1)	90.46(5)
N(2)–Ru–S(1)	86.55(4)
P–Ru–S(1)	168.920(15)
Si–Ru–S(1)	94.214(15)
C(1)–Ru–S(2)	94.20(5)
N(2)–Ru–S(2)	93.02(4)
P–Ru–S(2)	98.313(14)
Si–Ru–S(2)	162.959(16)
S(1)–Ru–S(2)	70.796(14)
O(2)–Si–C(11)	102.12(7)
O(2)–Si–C(21)	103.54(7)
C(11)–Si–C(21)	103.22(8)
O(2)–Si–Ru	101.00(4)
C(11)–Si–Ru	126.97(5)
C(21)–Si–Ru	116.60(6)

character in the C–O(bound to Ru) bond (1.239(5) Å) than there is in the C–O (bound to Si) bond (1.297(5) Å). This is consistent with valence bond structure **B** being more important than valence bond structure **A** (see Scheme 2). Thus a description of the chelate ligand as a tethered silyl ligand seems more appropriate than as a base-stabilised silylene ligand.

3. Conclusions

It has been demonstrated that the Si–Cl bond in the six-coordinate silyl complex, Ru(SiClPh₂)(κ²-S₂CNMe₂)(CO)(PPh₃)₂ (**2**) is reactive towards the three reagents, 2-hydroxypyridine, 2-aminopyridine, and thallium acetate, producing in each case mono-triphenylphosphine complexes containing tethered silyl ligands. Crystal structure determinations of Ru(κ²(Si,N)-Si-

Table 5
Selected bond lengths (Å) and angles (°) for **4**

<i>Bond lengths</i>	
Ru–C(1)	1.827(3)
Ru–N(3)	2.190(2)
Ru–P	2.3263(7)
Ru–Si	2.3400(7)
Ru–S(1)	2.4374(7)
Ru–S(2)	2.5189(7)
Si–N(2)	1.776(2)
Si–C(11)	1.889(3)
Si–C(21)	1.899(3)
S(1)–C(2)	1.714(3)
S(2)–C(2)	1.718(3)
O–C(1)	1.148(4)
N(1)–C(2)	1.326(3)
<i>Bond angles</i>	
C(1)–Ru–N(3)	173.10(10)
C(1)–Ru–P	91.32(9)
N(3)–Ru–P	92.29(6)
C(1)–Ru–Si	92.10(9)
N(3)–Ru–Si	81.52(6)
P–Ru–Si	99.04(2)
C(1)–Ru–S(1)	90.71(9)
N(3)–Ru–S(1)	86.68(6)
P–Ru–S(1)	170.66(2)
Si–Ru–S(1)	90.00(2)
C(1)–Ru–S(2)	94.00(9)
N(3)–Ru–S(2)	91.19(6)
P–Ru–S(2)	99.68(2)
Si–Ru–S(2)	160.15(3)
S(1)–Ru–S(2)	71.08(2)
N(2)–Si–C(11)	107.28(12)
N(2)–Si–C(21)	102.37(12)
C(11)–Si–C(21)	104.07(12)
N(2)–Si–Ru	98.50(8)
C(11)–Si–Ru	112.97(8)
C(21)–Si–Ru	129.23(9)

Ph₂OC₅H₄N)(κ²-S₂CNMe₂)(CO)(PPh₃) (**3**), Ru(κ²-(Si,N)-SiPh₂NHC₅H₄N)(κ²-S₂CNMe₂)(CO)(PPh₃) (**4**), and Ru(κ²(Si,O)-SiPh₂OCMeO)(κ²-S₂CNMe₂)(CO)-(PPh₃) (**5**) reveal a bonding situation within the five-membered rings which is intermediate between “tethered silyl” (predominant) and “base-stabilised silylene”.

4. Experimental

4.1. General procedures and instruments

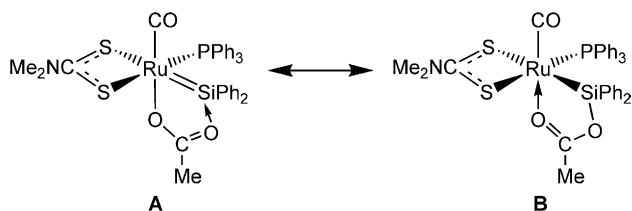
Standard laboratory procedures were followed as have been described previously [5]. The compound RuH(κ²-S₂CNMe₂)(CO)(PPh₃)₂ [3], was prepared by the literature method.

Infrared spectra (4000–400 cm⁻¹) were recorded as Nujol mulls between KBr plates on a Perkin–Elmer Paragon 1000 spectrometer. NMR spectra were obtained on either a Bruker DRX 400 or Bruker AC 200 at 25°C. For the Bruker DRX 400, ¹H and ¹³C NMR spectra

Table 6
Selected bond lengths (Å) and angles (°) for **5**

<i>Bond lengths</i>	
Ru–C(1)	1.801(5)
Ru–O(2)	2.182(3)
Ru–P	2.3386(12)
Ru–Si	2.3499(13)
Ru–S(1)	2.4249(12)
Ru–S(2)	2.4940(13)
Si–O(3)	1.775(3)
Si–C(21)	1.881(5)
Si–C(11)	1.888(5)
S(1)–C(4)	1.734(5)
S(2)–C(4)	1.707(5)
N–C(4)	1.338(6)
N–C(5)	1.441(8)
N–C(6)	1.504(8)
O(1)–C(1)	1.176(5)
O(2)–C(2)	1.239(5)
O(3)–C(2)	1.297(5)
C(2)–C(3)	1.508(6)
<i>Bond angles</i>	
C(1)–Ru–O(2)	172.3(2)
C(1)–Ru–P	90.69(15)
O(2)–Ru–P	94.69(9)
C(1)–Ru–Si	94.44(15)
O(2)–Ru–Si	79.09(9)
P–Ru–Si	100.94(5)
C(1)–Ru–S(1)	91.75(15)
O(2)–Ru–S(1)	84.00(9)
P–Ru–S(1)	169.09(5)
Si–Ru–S(1)	89.47(5)
C(1)–Ru–S(2)	101.39(15)
O(2)–Ru–S(2)	83.48(9)
P–Ru–S(2)	97.25(4)
Si–Ru–S(2)	155.67(5)
S(1)–Ru–S(2)	71.85(4)
O(3)–Si–C(21)	102.8(2)
O(3)–Si–C(11)	99.4(2)
C(21)–Si–C(11)	102.8(2)
O(3)–Si–Ru	98.59(11)
C(21)–Si–Ru	118.5(2)
C(11)–Si–Ru	129.48(15)
C(4)–S(1)–Ru	87.7(2)
C(4)–S(2)–Ru	86.1(2)
O(2)–C(2)–O(3)	123.9(4)
O(2)–C(2)–C(3)	119.7(4)
O(3)–C(2)–C(3)	116.3(4)
S(2)–C(4)–S(1)	114.0(3)

were obtained operating at 400.1 (^1H) and 100.6 (^{13}C) MHz, respectively. For the Bruker AC 200, ^1H and ^{13}C NMR spectra were obtained operating at 200.0



Scheme 2. Possible valence bond structures for $\text{Ru}(\kappa^2(\text{Si},\text{O})\text{-SiPh}_2\text{OC-MeO})(\kappa^2\text{-S}_2\text{CNMe}_2)(\text{CO})(\text{PPh}_3)$ (**5**).

(^1H) and 50.3 (^{13}C) MHz, respectively. Resonances are quoted in ppm and ^1H NMR spectra referenced to either tetramethylsilane (0.00 ppm) or the proteo-impurity in the solvent (7.25 ppm for CHCl_3). ^{13}C NMR spectra were referenced to CDCl_3 (77.00 ppm). Elemental analyses were obtained from the Microanalytical Laboratory, University of Otago.

4.2. Preparation of $\text{Ru}(\text{SiClPh}_2)(\kappa^2\text{-S}_2\text{CNMe}_2)(\text{CO})(\text{PPh}_3)_2$ (**2**)

HSiPh_2Cl (2.53 ml, 12.9 mmol) was added to a colourless solution of $\text{RuH}(\kappa^2\text{-S}_2\text{CNMe}_2)(\text{CO})(\text{PPh}_3)_2$ (1.00 g, 1.29 mmol) in toluene under nitrogen. The reaction mixture was heated to 85°C for 1.5 h. The resulting pale orange suspension was concentrated to approx. 2 ml and hexane was added to give pure **2** as a pale yellow solid which was collected and washed with hexane (1.20 g, 94%). Anal. Calc. for $\text{C}_{52}\text{H}_{46}\text{ClNOP}_2\text{RuS}_2\text{Si}$: C, 62.99; H, 4.68; N, 1.41. Found: C, 62.78; H, 4.71; N, 1.43%. IR (cm^{-1}): 1915s $\nu(\text{CO})$. ^1H NMR (CDCl_3 , δ): 2.16 (s, 3H, NMe_2), 2.35 (s, 3H, NMe_2), 6.99–7.58 (m, 40H, SiPh_2 and PPh_3). ^{13}C NMR (CDCl_3 , δ): 38.1 (NMe_2), 127.6 (t' [5], $^2,4J_{\text{CP}}=9.0$ Hz, $o\text{-C}_6\text{H}_5$), 128.2 (SiPh_2), 128.7 (SiPh_2), 129.6 (s, $p\text{-C}_6\text{H}_5$), 132.9 (m, $i\text{-C}_6\text{H}_5$), 134.4 (t' , $^3,5J_{\text{CP}}=10.0$ Hz, $m\text{-C}_6\text{H}_5$), 178.1 (m, CO), 210.3 (S_2CNMe_2) (some coupling constants were not resolved).

4.3. Preparation of $\text{Ru}(\kappa^2(\text{Si},\text{N})\text{-SiPh}_2\text{OC}_5\text{H}_4\text{N})(\kappa^2\text{-S}_2\text{CNMe}_2)(\text{CO})(\text{PPh}_3)$ (**3**)

$\text{Ru}(\text{SiPh}_2\text{Cl})(\kappa^2\text{-S}_2\text{CNMe}_2)(\text{CO})(\text{PPh}_3)_2$ (173.5 mg, 0.175 mmol) and 2-hydroxypyridine (33.3 mg, 0.35 mmol) were added to benzene (20 ml) under nitrogen. The white suspension was stirred for 1 h and then filtered through Celite. The filtrate was concentrated and hexane added to give a white solid. The crude product was dissolved in CH_2Cl_2 and purified by chromatography on silica gel using CH_2Cl_2 /hexane ($v/v=1:1$) as eluent. A white solid was obtained from the second colourless fraction, which was recrystallised from CH_2Cl_2 and heptane to give pure **3** as colourless crystals (77 mg, 56%). Anal. Calc. for $\text{C}_{39}\text{H}_{35}\text{N}_2\text{O}_2\text{PRuS}_2\text{Si}$: C, 58.82; H, 4.55; N, 3.61. Found: C, 58.58; H, 4.38; N, 3.43%. IR (cm^{-1}): 1915 $\nu(\text{CO})$. ^1H NMR (CDCl_3 , δ): 3.03 (s, 3H, NMe_2), 3.24 (s, 3H, NMe_2), 6.31–6.34 (m, 1H, $\text{OC}_5\text{H}_4\text{N}$), 6.89–7.45 (m, 25H, SiPh_2 and PPh_3), 7.72 (apparent dd, 2H, $J=1.1$ Hz, 7.8 Hz, $\text{OC}_5\text{H}_4\text{N}$), 8.07 (apparent dd, 2H, $J=1.8$, 5.8 Hz, $\text{OC}_5\text{H}_4\text{N}$). ^{13}C NMR (CDCl_3 , δ): 38.6 (NMe_2), 39.1 (NMe_2), 112.2 ($\text{OC}_5\text{H}_4\text{N}$), 115.6 ($\text{OC}_5\text{H}_4\text{N}$), 126.8 (SiPh_2), 126.9 (SiPh_2), 127.5 (SiPh_2), 127.7 (d, $^2J_{\text{CP}}=9.1$ Hz, $o\text{-C}_6\text{H}_5\text{P}$), 129.0 ($p\text{-C}_6\text{H}_5\text{P}$), 132.8 (SiPh_2), 133.0 (SiPh_2), 133.1 (d, $^3J_{\text{CP}}=10.1$ Hz, $m\text{-C}_6\text{H}_5\text{P}$), 134.5 (d, $^1J_{\text{CP}}=42.3$ Hz, $i\text{-C}_6\text{H}_5\text{P}$), 139.1 ($\text{OC}_5\text{H}_4\text{N}$), 143.6

(SiPh₂), 143.9 (SiPh₂), 148.4 (OC₅H₄N), 167.1 (OC₅H₄N), 204.6 (CO), 212.5 (S₂CNMe₂). Coupling constant for CO not resolved.

4.4. Preparation of Ru(κ^2 (Si,N)-SiPh₂NHC₅H₄N)(κ^2 -S₂CNMe₂)(CO)(PPh₃) (**4**)

Ru(SiPh₂Cl)(κ^2 -S₂CNMe₂)(CO)(PPh₃)₂ (198 mg, 0.20 mmol) and 2-aminopyridine (39 mg, 0.42 mmol) were added to benzene (20 ml) under nitrogen. The orange mixture turned to a yellow suspension and after stirring for 16 h it was filtered through Celite. The yellow filtrate was evaporated to low volume and hexane added to give pale yellow solid. This was dissolved in CH₂Cl₂ and subjected to thin-layer chromatography on silica gel using CH₂Cl₂/hexane (v/v=1:1) as eluent. From the second colourless band was obtained an off-white solid, which was recrystallised from CH₂Cl₂ and heptane to give pure **4** as colourless crystals (78 mg, 50%). Anal. Calc. for C₃₉H₃₆N₃OPRuS₂Si·1/4CH₂Cl₂: C, 58.85; H, 4.68; N, 5.28. Found: C, 58.59; H, 4.60; N, 5.24%. IR (cm⁻¹): 1925 vs ν (CO). ¹H NMR (CDCl₃, δ): 3.02 (s, 3H, NMe₂), 3.21 (s, 3H, NMe₂), 5.15 (s, 1H, NHpy), 6.07 (apparent dt, 1H, *J*=1.1, 6.5 Hz, C₅H₄N), 6.60 (apparent d, 1H, *J*=8.2 Hz, C₅H₄N), 6.87–6.90 (m, 2H, SiPh₂), 6.95–6.98 (m, 1H, C₅H₄N), 7.07–7.37 (m, 21H, SiPh₂ and PPh₃), 7.72 (apparent dd, 2H, *J*=1.3, 8.0 Hz, SiPh₂), 8.11 (apparent dd, 1H, *J*=1.6, 6.0 Hz, C₅H₄N). ¹³C NMR (CDCl₃, δ): 38.5 (NMe₂), 39.1 (NMe₂), 110.6 (C₅H₄N), 111.8 (C₅H₄N), 127.0 (SiPh₂), 127.1 (SiPh₂), 127.1 (SiPh₂), 127.2 (SiPh₂), 127.6 (d, ²*J*_{CP}=9.1 Hz, *o*-C₆H₅P), 128.9 (*p*-C₆H₅P), 133.3 (d, ³*J*_{CP}=10.1 Hz, *m*-C₆H₅P), 133.7 (SiPh₂), 133.8 (SiPh₂), 134.7 (d, ¹*J*_{CP}=42.3 Hz, *i*-C₆H₅P), 137.1 (C₅H₄N), 143.9 (SiPh₂), 144.9 (SiPh₂), 149.4 (C₅H₄N), 165.1 (C₅H₄N), 204.9 (d, ²*J*_{CP}=16.1 Hz, CO), 212.5 (S₂CNMe₂).

4.5. Preparation of Ru(κ^2 (Si,O)-SiPh₂OCMeO)(κ^2 -S₂CNMe₂)(CO)(PPh₃) (**5**)

Ru(SiPh₂Cl)(κ^2 -S₂CNMe₂)(CO)(PPh₃)₂ (235 mg, 0.24 mmol) and thallium acetate (140 mg, 0.48 mmol) were added to CH₂Cl₂ (20 ml). The orange mixture turned to a white suspension upon stirring. This was stirred for 2 h and then filtered through Celite. The colourless filtrate was evaporated to a low volume and hexane was added to give a white solid. This was recrystallised from CH₂Cl₂/hexane to give pure **5** as colourless crystals (128 mg, 68%). Anal. Calc. for C₃₆H₃₄NO₃PRuS₂Si_{1.5}CH₂Cl₂: C, 52.10; H, 4.15; N, 1.56. Found: C, 52.05; H, 4.34; N, 1.69. IR (cm⁻¹): 1909 vs ν (CO); 1604 (O₂CMe). ¹H NMR (CDCl₃, δ): 1.97 (s, 3H, O₂CCH₃), 3.13 (s, 3H, NMe₂), 3.21 (s, 3H, NMe₂), 6.95–7.01 (m, 5H, SiPh₂), 7.23–7.38 (m, 17H, SiPh₂ and PPh₃), 7.72–7.76 (m, 3H, SiPh₂). ¹³C

NMR (CDCl₃, δ): 21.4 (O₂CCH₃), 38.5 (NMe₂), 39.0 (NMe₂), 127.1 (SiPh₂), 127.4 (SiPh₂), 127.7 (d, ²*J*_{CP}=10.1 Hz, *m*-C₆H₅P), 128.4 (SiPh₂), 128.9 (SiPh₂), 129.4 (s, *p*-C₆H₅P), 133.3 (SiPh₂), 133.8 (d, ³*J*_{CP}=11.1 Hz, *m*-C₆H₅P), 133.9 (SiPh₂), 141.0 (SiPh₂), 144.2 (SiPh₂), 182.4 (O₂CCH₃), 204.7 (d, ²*J*_{CP}=16.1 Hz, CO), 213.1 (S₂CNMe₂).

4.6. X-ray crystal structure determinations for complexes **1–5**

X-ray data collection was by Siemens SMART diffractometer with a CCD area detector at 150 K using graphite monochromated Mo K α radiation (λ =0.71073 Å). Data were integrated and corrected for Lorentz and polarisation effects using SAINT [6] software. Semi-empirical absorption corrections were applied based on equivalent reflections using SADABS [7]. The structures were solved by Patterson and Fourier methods and refined by full-matrix least squares on *F*² using programs SHELXS [8] and SHELXL [9]. All non-hydrogen atoms were refined anisotropically. Hydrogen atoms were located geometrically and refined using a riding model with thermal parameter 20% greater than *U*_{iso} of the carrier atom. The benzene molecules of solvation in **3** were ordered. The final electron density map for **5** revealed one ordered dichloromethane of solvation and in addition, contained numerous electron density peaks clustered in one region of the unit cell, which could not be resolved sensibly into a molecule and presumably represent additional disordered dichloromethane of solvation. This density was removed using the “squeeze” function of PLATON [10] before the final refinement. Crystal data and refinement details are given in Table 1.

5. Supplementary material

Crystallographic data (excluding structure factors) for the structures reported have been deposited with the Cambridge Crystallographic Data Centre as Supplementary Publication Nos. 234040–234044 for **1–5**, respectively. Copies of this information can be obtained free of charge from the Director, CCDC, 12 Union Road, Cambridge, CB2 1EZ, UK (fax: +44-1223-336-033; e-mail: deposit@ccdc.cam.ac.uk or www: <http://www.ccdc.cam.ac.uk>).

Acknowledgement

We thank the Marsden Fund administered by the Royal Society of NZ for supporting this work. We also thank the Croucher Foundation, Hong Kong, for

support and for granting a Postdoctoral Fellowship to H-WK. We also thank the University of Auckland Research Committee for partial support of this work through grants-in-aid.

References

- [1] (a) W. Malisch, *Chem. Ber.* 107 (1974) 3835;
(b) G. Thum, W. Ries, D. Greissing, W. Malisch, *J. Organomet. Chem.* 252 (1983) C67;
(c) G.R. Clark, C.E.F. Rickard, W.R. Roper, D.M. Salter, L.J. Wright, *Pure Appl. Chem.* 62 (1990) 1039;
(d) C.E.F. Rickard, W.R. Roper, D.M. Salter, L.J. Wright, *J. Am. Chem. Soc.* 114 (1992) 9682;
(e) W. Adam, U. Azzena, F. Prechtel, K. Hindahl, W. Malisch, *Chem. Ber.* 125 (1992) 1409;
(f) W. Malisch, S. Möller, O. Fey, H.-U. Wekel, R. Pikel, U. Posset, W. Kiefer, *J. Organomet. Chem.* 507 (1996) 117;
(g) K. Hübler, P.A. Hunt, S.M. Maddock, C.E.F. Rickard, W.R. Roper, D.M. Salter, P. Schwerdtfeger, L.J. Wright, *Organometallics* 16 (1997) 5076;
(h) J.S. McIndoe, B.K. Nicholson, *J. Organomet. Chem.* 648 (2002) 237.
- [2] W. Malisch, S. Möller, R. Lankat, J. Reising, S. Schmitzer, O. Fey, in: N. Auner, J. Weiss (Eds.), *Organosilicon Chemistry II* From Molecules to Materials, VCH, Weinheim, Germany, 1996, p. 575.
- [3] P.B. Critchlow, S.D. Robinson, *J. Chem. Soc., Dalton Trans.* (1975) 1367.
- [4] (a) K. Osakada, S. Sarai, T. Koizumi, T. Yamamoto, *Organometallics* 16 (1997) 3973;
(b) M. Tanabe, K. Osakada, *Chem. Lett.* (2001) 962;
(c) H. Sakaba, T. Hirata, C. Kabuto, H. Hirino, *Chem. Lett.* (2001) 1078;
(d) A. Berenbaum, A.J. Lough, I. Manners, *Acta Crystallogr. E* 58 (2002) 679;
(e) D.G. Gusev, F.-G. Fontaine, A.J. Lough, D. Zargarain, *Angew. Chem., Int. Ed. Engl.* 42 (2003) 216;
(f) G.I. Nikonov, P. Mountford, S.R. Dubberley, *Inorg. Chem.* 42 (2003) 258.
- [5] S.M. Maddock, C.E.F. Rickard, W.R. Roper, L.J. Wright, *Organometallics* 15 (1996) 1793.
- [6] SAINT, Area detector integration software, Siemens Analytical Instruments Inc., Madison, WI, USA, 1995.
- [7] G.M. Sheldrick, SADABS, Program for semi-empirical absorption corrections, University of Göttingen, Göttingen, Germany, 1997.
- [8] G.M. Sheldrick, SHELXS, Program for crystal structure determination, University of Göttingen, Göttingen, Germany, 1997.
- [9] G.M. Sheldrick, SHELXL, Program for crystal structure refinement, University of Göttingen, Göttingen, Germany, 1997.
- [10] A.L. Spek, *Acta Crystallogr. A* 46 (1990) C34.